Article

Stepwise Noncovalent Synthesis Leading to Dendrimer-Based Assemblies in Water

Thomas M. Hermans, Maarten A. C Broeren, Nikos Gomopoulos, A. F. Smeijers, Brahim Mezari, Ellen N. M. Van Leeuwen, Matthijn R. J. Vos, Pieter C. M. M. Magusin, Peter A. J. Hilbers, Marcel H. P. Van Genderen, Nico A. J. M. Sommerdijk, George Fytas, and Meijer

J. Am. Chem. Soc., **2007**, 129 (50), 15631-15638 • DOI: 10.1021/ja074991t

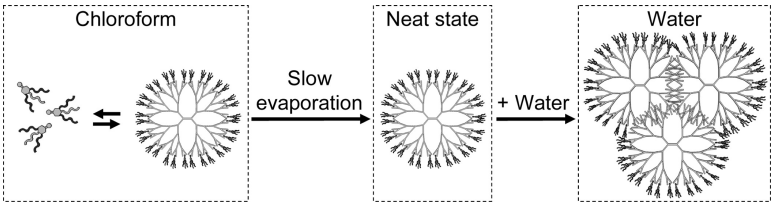

More About This Article

Additional resources and features associated with this article are available within the HTML version:

- Supporting Information
- Links to the 5 articles that cite this article, as of the time of this article download
- Access to high resolution figures
- Links to articles and content related to this article
- Copyright permission to reproduce figures and/or text from this article

View the Full Text HTML

J|A|C|S
ARTICLES
Published on Web 11/21/2007

Stepwise Noncovalent Synthesis Leading to Dendrimer-Based Assemblies in Water

Thomas M. Hermans,[†] Maarten A. C Broeren,[†] Nikos Gomopoulos,[‡] A. F. Smeijers,[§] Brahim Mezari,[||] Ellen N. M. Van Leeuwen,[⊥] Matthijn R. J. Vos,[⊥] Pieter C. M. M. Magusin,[||] Peter A. J. Hilbers,[§] Marcel H. P. Van Genderen,[†] Nico A. J. M. Sommerdijk,[⊥] George Fytas,[‡] and E.W. Meijer*[,†]

Contribution from the Laboratory of Macromolecular and Organic Chemistry, Biomodeling and Bioinformatics, Laboratory of Inorganic Chemistry and Catalysis, and Soft Matter CryoTEM Research Unit, Eindhoven University of Technology, P.O. Box 513, 5600 MB Eindhoven, The Netherlands, and Department of Materials Science and Technology, University of Crete and FORTH, P.O. Box 1527, 71110 Heraklion, Greece

Received July 24, 2007; E-mail: E.W.Meijer@tue.nl

Abstract: We provide detailed insight into complex supramolecular assembly processes by fully characterizing a multicomponent model system using dynamic light scattering, cryogenic transmission electron microscopy, atomic force microscopy, and various NMR techniques. First, a preassembly of a host molecule (the fifth-generation urea-adamantyl poly(propylene imine) dendrimer) and 32 guest molecules (a water- and chloroform-soluble ureidoacetic acid guest) was made in chloroform. The association constant in chloroform is concealed by guest self-association and is therefore higher than 10^3 M^{-1}. Via the neat state the single-host complex was transferred to water, where larger dendrimer-based assemblies were formed. The core of these assemblies, consisting of multiple host molecules (on average three), is kinetically trapped upon dissolution in water, and its size is constant irrespective of the concentration. The guest molecules forming the corona of the assemblies, however, stay dynamic since they are still in rapid exchange on the NMR time scale, as they were in chloroform. A stepwise noncovalent synthesis provides a means to obtain metastable dynamic supramolecular assemblies in water, structures that cannot be formed in one step.

Introduction

The noncovalent synthesis of supramolecular complexes is at the heart of current research in nanonscience.[1] Today, most supramolecular structures are made by self-assembly of the molecules used in the process, and in most cases the thermodynamically favored product is formed. More recently, also kinetically trapped species have been observed.[2] An intriguing next step is to synthesize supramolecular assemblies in solvents in which the individual components are not soluble.[3,4] Then a more sophisticated fabrication process should be used, as beautifully illustrated by the formation of liposomes and vesicles.[5] However, next to these structures, the examples of the stepwise noncovalent synthesis of supramolecular architectures are very limited. Dendrimers are in our view excellent building blocks to study this new area of noncovalent synthesis. They are monodisperse, have a highly branched and regular structure,[6] and have been used for the construction of supramolecular assemblies in organic solvents[7] and in water.[8] These assemblies have potential applications in the fields of drug delivery,[9] gene transfection,[10] and imaging[11] and as extractants.[12] In aqueous solutions, covalent modification of the periphery, combined with the flexibility of the dendrimer core, often leads

[†] Laboratory of Macromolecular and Organic Chemistry, Eindhoven University of Technology.
[‡] University of Crete and FORTH.
[§] Biomodeling and Bioinformatics, Eindhoven University of Technology.
[||] Laboratory of Inorganic Chemistry and Catalysis, Eindhoven University of Technology.
[⊥] Soft Matter CryoTEM Research Unit, Eindhoven University of Technology.

(1) Lehn, J.-M. *Science* **2002**, *295*, 2400−2403. Reinhoudt, D. N.; Crego-Calama, M. *Science* **2002**, *295*, 2403−2407. Kato, T. *Science* **2002**, *295*, 2414−2418. Whitesides, G. M.; Grybowski, B. *Science* **2002**, *295*, 2418−2421.
(2) Mukhopadhyay, P.; Zavalij, P. Y.; Isaacs, L. *J. Am. Chem. Soc.* **2006**, *128*, 14093−14102.
(3) Broeren, M. A. C.; Linhardt, J. G.; Malda, H.; de Waal, B. F. M.; Versteegen, R. M; Meijer, J. T.; Löwik, D. W. P. M.; Hest, J. C. M. v.; Genderen, M. H. P. v.; Meijer, E. W. *J. Polym. Sci., A* **2005**, *43*, 6431−6437.
(4) Chun, D.; Wudl, F.; Nelson, A. *Macromolecules* **2007**, *40*, 1782−1785.
(5) Mui, B.; Chow, L.; Hope, M. J. *Methods Enzymol.* **2003**, *367*, 3−14. Düzgüne_, N. *Methods Enzymol.* **2003**, *367*, 23−27.
(6) Bosman, A. W.; Janssen, H. M.; Meijer, E. W. *Chem. Rev.* **1999**, *99*, 1655−1688. Fréchet, J. M. J. *J. Polym. Sci., A* **2003**, *41*, 3713−3725. Newkome, G. R.; Moorefield, C. N.; Vögtle, F. *Dendrimers and Dendrons: Concepts, Synthesis, Applications*; Wiley-VCH, Weinheim, Germany, 2001. Tomalia, D. A.; Naylor, A. M.; Goddard, W. A., III. *Angew. Chem.* **1990**, *102*, 119−157. Fréchet, J. M. J. *Science* **1994**, *263*, 1710−1715. Voit, B. I. *Acta Polym.* **1995**, *46*, 87−99.
(7) Zimmerman, S. C.; Wang, Y.; Bharathi, P.; Moore, J. S. *J. Am. Chem. Soc.* **1998**, *120*, 2172−2173. Newkome, G. R.; Woosley, B. D.; He, E.; Moorefield, C. N.; Güther, R.; Baker, G. R.; Escamilla, G. H.; Merrill, J.; Luftmann, H. *Chem. Commun.* **1996**, 2737−2738.
(8) Bakshi, M. S.; Sood, R.; Ranganathan, R.; Shin, P. *Colloid Polym. Sci.* **2005**, *284*, 58−65. Li, Y.; McMillan, C. A.; Bloor, D. M.; Penfold, J.; Warr, J.; Holzwarth, J. F.; Wyn-Jones, E. *Langmuir* **2000**, *16*, 7999−8004. Wang, C.; Wyn-Jones, E.; Sidhu, J.; Tam, K. C. *Langmuir* **2007**, *23*, 1635−1639.
(9) Boas, U.; Heegaard, P. M. H. *Chem. Soc. Rev.* **2004**, *33*, 43−63. Gillies, E. R.; Fréchet, J. M. J. *Drug Discovery Today* **2005**, *10*, 35−43.

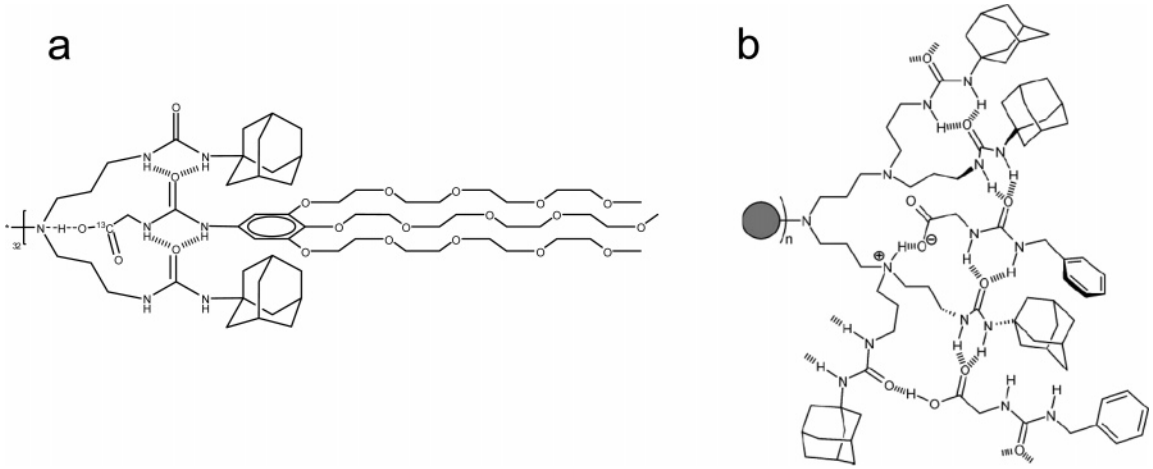

Figure 1. (a) Initial pincer model for a urea-adamantyl-modified fifth-generation poly(propylene imine) dendrimer with an associated ureidoacetic acid guest molecule having an acid−base interaction, yielding a tight ion pair, and multiple hydrogen-bonding interactions in chloroform. (b) A more realistic model based on X-ray crystallography and molecular dynamics studies. Reprinted with permission from ref 17. Copyright 2007 Wiley-VCH.

to surfactant-like behavior and assemblies that are associated with such amphiphilic molecules.[13] The periphery of a dendrimer can also be modified in a noncovalent way, by using host−guest interactions (e.g., surfactants[14] or cyclodextrins[15]). Previously, we have reported on a system based on supramolecular guest−host chemistry using urea-adamantyl-functionalized poly(propylene imine) dendrimers (generations 1−5), combined with ureidoacetic acid guest molecules.[16] In one of our recent systems, we used the fifth-generation dendrimer (host) and a ureidoacetic acid molecule (guest) with oligoethylene glycol tails for solubility (Figure 1). Recently, Chang et al. refined the initial pincer model (Figure 1a) using X-ray crystallography and molecular dynamics simulations (Figure 1b).[17]

This system was investigated extensively in the gas phase[18] and in chloroform solution.[19] The first preliminary results indicated that using a stepwise approach the single-host complex

Scheme 1 [a]

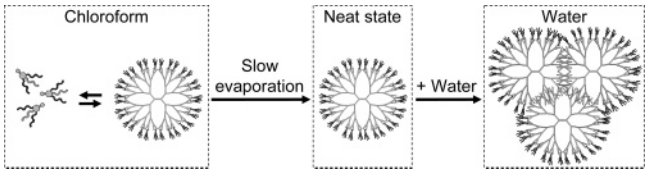

[a] First, a complex is made by mixing the guest and host together in chloroform with a ratio of 32 to obtain a single-host complex. Next, the chloroform is evaporated with a gentle nitrogen flow, and the resulting thin film is dried in vacuo and subsequently dissolved in ultrapure water, yielding small dendrimer-based assemblies.

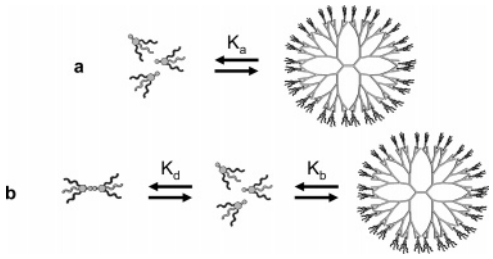

Figure 2. Models for the binding of the guest molecule to the dendrimer. Model a was reported by us previously. In this model there is one equilibrium, i.e., the binding of the guest to the host with an apparent association constant K_a (400 ± 95 M^{-1}). Model b takes into account the dimerization of the guest molecule and is explained in more detail in the text. K_d is the dimerization constant, and K_b is the apparent association constant for the binding of the monomeric guest to the host according to model b.

(a single host and multiple guest molecules, left in Scheme 1) could be transferred to water.[3] In the present paper we show a detailed characterization of the different stages of the approach we refer to as stepwise noncovalent synthesis and demonstrate that during this process the single-host complexes present in chloroform transform to small assemblies of about three host molecules stabilized by the guest molecules at the periphery (Scheme 1).

We present the detailed analysis of the stepwise procedure, provide a detailed analysis of the system in chloroform, and investigate the neat state and the subsequent small dendrimer-based assemblies obtained in water. DLS (dynamic light scattering), cryo-TEM (cryogenic transmission electron microscopy), AFM (atomic force microscopy), and various NMR

(10) Tang, M. X.; Redemann, C. T.; Szoka, F. C., Jr. *Bioconjugate Chem.* **1996**, *7*, 703−714. Bielinska, A.; Kukowska-Latallo, J. F.; Johnson, J.; Tomalia, D. A.; Baker, J. R. *Nucleic Acids Res.* **1996**, *24*, 2176−2182. Zhou, J.; Wu, J.; Hafdi, N.; Behr, J.-P.; Erbacher, P.; Peng, L. *Chem. Commun.* **2006**, 2362−2364.
(11) Tóth, E.; Pubanz, D.; Vauthey, S.; Helm, L.; Mehrbach, A. E. *Chem.−Eur. J.* **1996**, *2*, 1607−1615. Langereis, S. L.; de Lussanet, Q. G.; Genderen, M. H. P. v.; Backes, W. H.; Meijer, E. W. *Macromolecules* **2004**, *37*, 3084−3091.
(12) Morara, A. D.; McCarley, R. L. *Org. Lett.* **2006**, *8*, 1999−2002. Sayed-Sweet, Y.; Hedstrand, D. M; Spinder, R.; Tomalia, D. A. *J. Mater. Chem.* **1997**, *7*, 1199−1205.
(13) Schenning, A. P. H. J.; Elissen-Román, C.; Weener, J.-W.; Baars, M. W. P. L.; Gaast, S. J. v. d.; Meijer, E. W. *J. Am. Chem. Soc.* **1998**, *120*, 8199−8208. Li, X.; Imae, T.; Leisner, D.; López-Quintela, M. A. *J. Phys. Chem. B* **2002**, 12170−12177. Donners, J. J. J. M.; Heywood, B. R.; Meijer, E. W.; Nolte, R. J. M.; Sommerdijk, N. A. J. M. *Chem.−Eur. J.* **2002**, *8*, 2561−2567.
(14) Miyazaki, M.; Torigoe, K.: Esumi, K. *Langmuir* **2000**, *16*, 1522−1528. Esumi, K.; Kuwabara, K.; Chiba, T.; Kobayashi, F.; Mizutani, H.; Torigoe, K. *Colloids Surf.* **2002**, *197*, 141−146.
(15) Michels, J. J.; Baars, M. W. P. L.; Meijer, E. W.; Huskens, J.; Reinhoudt, D. N. *J. Chem. Soc., Perkin Trans. 2* **2000**, 1914−1918.
(16) Baars, M. W. P. L.; Karlsson, A. J.; Sorokin, V.; de Waal, B. F. W.; Meijer, E. W. *Angew. Chem., Int. Ed.* **2000**, *39*, 4262−4265. Pittelkow, M.; Christensen, J. B.; Meijer, E. W. *J. Polym. Sci., A* **2004**, *42*, 3792−3799.
(17) Chang, T.; Pieterse, K.; Broeren, M. A. C.; Kooijman, H.; Spek, A. L.; Hilbers, P. A. J.; Meijer, E. W. *Chem.−Eur. J.* **2007**, *13*, 7883−7889.
(18) Broeren, M. A. C.; van Dongen, J. L. J.; Pittelkow, M.; Christensen, J. B.; Genderen, M. H. P. v.; Meijer, E. W. *Angew. Chem., Int. Ed.* **2004**, *43*, 3557−3562. Pittelkow, M.; Nielsen, C. B.: Broeren, M. A. C.: van Dongen, J. L. J.; Genderen, M. H. P. v.; Meijer, E. W.; Christensen, J. B. *Chem.−Eur. J.* **2005**, *11*, 5126−5135.
(19) Broeren, M. A. C.; Waal, B. F. M. d.; Genderen, M. H. P. v.; Sanders, H. M. H. F.; Fytas, G.; Meijer, E. W. *J. Am. Chem. Soc.* **2005**, *127*, 10334−10343. Banerjee, D.; Broeren, M. A. C.; Genderen, M. H. P. v.; Meijer, E. W.; Rinaldi, P. L. *Macromolecules* **2004**, *37*, 8313−8318.

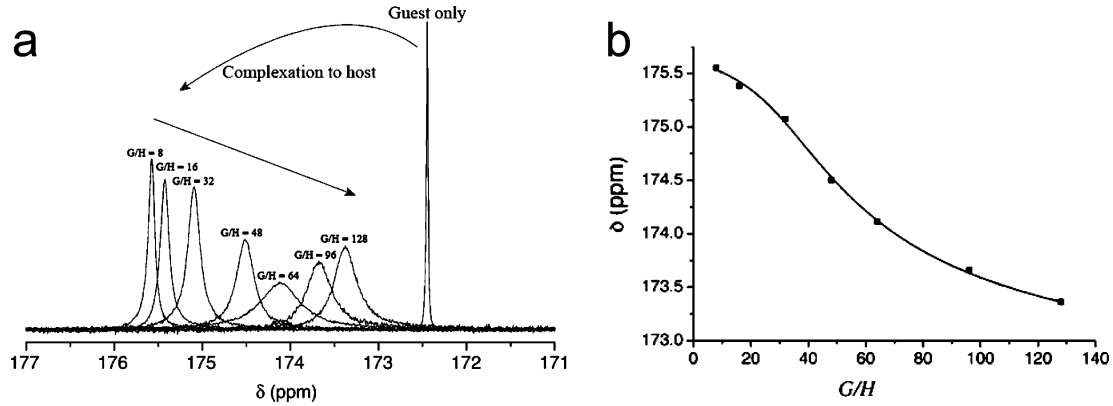

Figure 3. (a) ^{13}C NMR spectra of different guest/host ratios (G/H). The ^{13}C-labeled carboxyl moiety of the guest molecule shifts downfield upon binding to the host and shifts back to the unbound chemical shift (172.5 ppm) when the guest/host ratio is increased. The concentration of the guest was kept constant at 2.46×10^{-2} M. (b) The observed chemical shift is plotted as a function of the guest/host ratio (G/H). The solid line represents the fit obtained when noncooperative binding is assumed ($K_a = 400 \pm 95$ M^{-1}).

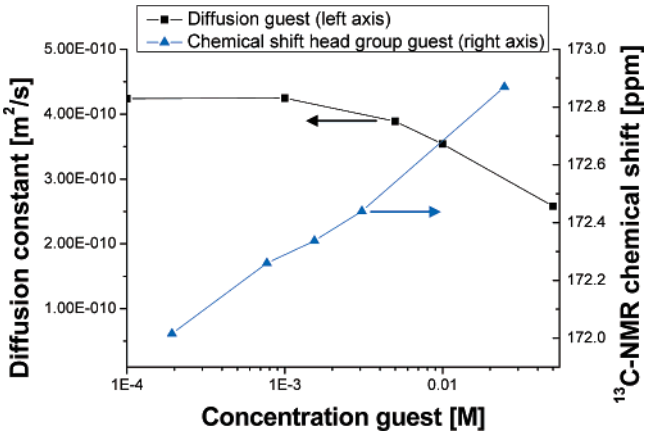

Figure 4. Guest molecule on its own at different concentrations in chloroform. The diffusion of the guest molecule was measured using ^{1}H DOSY NMR (left axis), and the chemical shift was obtained by ^{13}C NMR (right axis). The hydrodynamic radius (R_H) was calculated from the diffusion constants using the Stokes−Einstein equation. At the lowest concentration (10^{-4} M) R_H is 0.58 nm, and at the highest concentration (5×10^{-2} M) R_H is 0.95 nm.

(nuclear magnetic resonance) techniques were used to confirm the procedure presented in Scheme 1.

Results and Discussion

System in Chloroform. Earlier, we described the binding of the guest molecule to the host in chloroform as depicted in Figure 2a.[19] In chloroform, the host is molecularly dissolved and has a hydrodynamic radius (R_H) of 2.2 nm.[20] Upon binding of on average 32 guest molecules, R_H increases to 3.0 nm, implying the formation of a single-host complex composed of one dendrimer and multiple guest molecules. The acid−base interaction (Figure 1) was monitored using ^{13}C NMR spectroscopy (Figure 3a). The ^{13}C-labeled carboxyl moiety gave rise to a single peak, demonstrating that the equilibrium between bound and unbound guest is fast on the NMR time scale (<2.4 ms). The apparent association constant ($K_a = 400 \pm 95$ M^{-1}) and the number of binding sites (41) were calculated by fitting a noncooperative binding model (Figure 3b).

The concentration dependency of the chemical shift of the carboxyl moiety indicated, however, that at 2.46×10^{-2} M (concentration in the titration experiment) the guest is not molecularly dissolved (▲ in Figure 4). ^{1}H DOSY (diffusion-ordered spectroscopy) NMR showed that the diffusion constant of the guest molecules decreased by less than a factor of 2 compared to the molecularly dissolved state (■ in Figure 4). This implies the formation of dimers of guest molecules (Figure 2b), most probably through interactions of the carboxyl moieties.

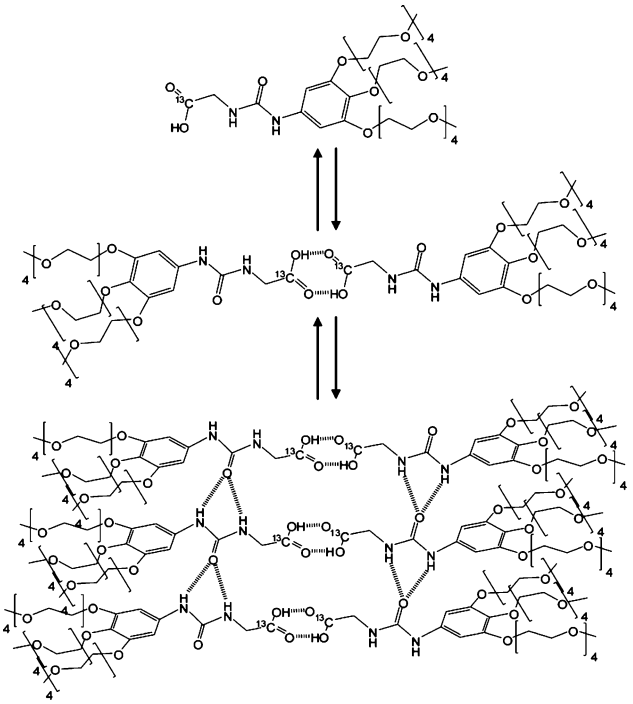

Figure 5. The guest molecule can dimerize, and the dimers can possibly stack into larger assemblies.

Fitting the ^{13}C NMR shifts of the guest molecule's carboxyl moieties to a dimerization equilibrium yielded a dimerization constant (K_d) of 200 ± 200 M^{-1} (see the Supporting Information). From this fit it follows that at 2.46×10^{-2} M 73% of the guest is dimerized, causing the effective concentration of the monomeric guest to be lower than the nominal value. In contrast, using model b, the apparent association constant K_b was found to be approximately 2000 M^{-1} (Figure 6a).[21] However, on the

(20) Versteegen, R. M.; van Beek, D. J. M.; Sijbesma, R. P.; Vlassopoulos, D.; Fytas, G.; Meijer, E. W. *J. Am. Chem. Soc.* **2005**, *127*, 13862−13868.

(21) Attempts to fit model b to the data failed; therefore, simulations were performed to get an estimation of the apparent association constant K_b.

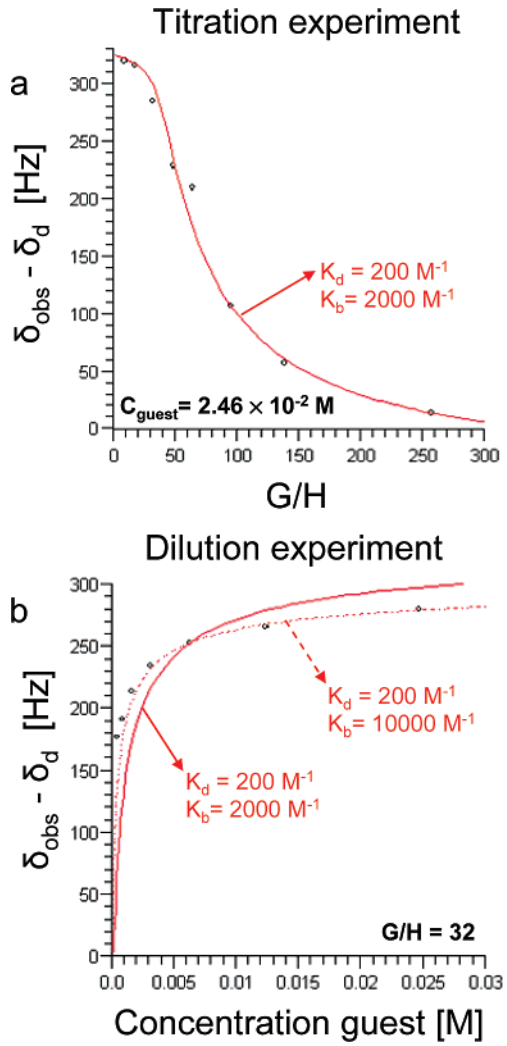

Figure 6. (a) Titration experiment: difference between the observed chemical shift (δ_{obsd}) and the chemical shift of the dimer (δ_d) versus the guest/host ratio (G/H). The concentration of the guest is constant at 2.46 × 10^{-2} M. The dimerization and binding are taken into account (model b). The open circles are the data points, and the solid line is simulated. (b) Dilution experiment: $\delta_{obsd} - \delta_d$ is plotted versus the concentration of the guest (the guest/host ratio is constant at 32). The solid line represents the simulation, keeping the same parameters as for the titration experiment (a), and the dashed line is found when K_b is increased to 10^4 M^{-1}.

basis of the structure of the guest molecule, dimerization is not expected to be the only possible pathway to guest assembly. The urea moieties present are likely to form lateral hydrogen-bonding arrays (Figure 5) as was demonstrated in a single-crystal X-ray structure by Zhao[22] and co-workers using ureylenedicarboxylic acid model compounds.

The presence of higher order assemblies would further decrease the effective concentration of the monomeric guest. To investigate this hypothesis, the guest−host system was diluted (G/H = 32, from 2.46 × 10^{-2} to 10^{-4} M), thereby driving the guest to its monomeric form. The amount of higher order guest assemblies will be negligible, and the dominant equilibrium will be the guest association, when the association is the strongest interaction. Remarkably, the ^{13}C NMR chemical shifts did not change as much as was expected (Figure 6b) on the basis of association constants of 400 or even 2000 M^{-1},

(22) Zhao, X.; Chang, Y.-L.; Fowler, F. W.; Lauher, J. W. *J. Am. Chem. Soc.* **1990**, *112*, 6627−6634.

Scheme 2 [a]

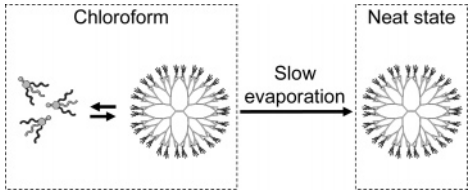

[a] After the precomplexation in solution, the chloroform is gently evaporated, leaving a thin film behind.

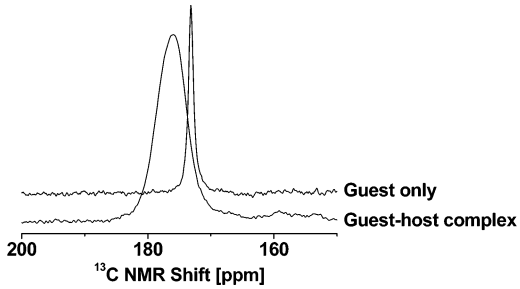

Figure 7. Carboxyl region in the MAS ^{13}C NMR spectrum of the guest and guest−host complex (G/H = 32) showing the downfield shift of the ^{13}C-labeled carboxyl moiety (upper spectrum, 173 ppm and a line width of 120 Hz; lower spectrum, 175 ppm and a line width of 670 Hz) upon binding to the host.

implying a higher fraction of bound guest molecules than predicted. Figure 6a shows that the titration can be nicely simulated to match the data, but if the same parameters (e.g., K_d and K_b) are used to simulate the dilution experiment, the match is poor (Figure 6b).

Apparently, the association constant of the guest is higher than 2000 M^{-1}. When simulated using model b (even though we know the model is incomplete), an association constant of ~10^4 M^{-1} was required to match the observed chemical shifts (Figure 6b). Clearly, dimerization of the carboxyl moieties insufficiently describes this process. Nevertheless, these results show that a high association constant can be concealed by self-association of the guest molecules.[23]

Neat State. Going from chloroform to the neat state is the next undertaking in the stepwise noncovalent synthetic procedure (Scheme 2). During the evaporation, the equilibrium will shift completely to the bound state for the guest molecules. The resulting thin film was investigated by magic-angle spinning (MAS) ^{1}H and ^{13}C NMR spectroscopy. Compared to the ^{13}C NMR spectrum of the guest alone, a downfield shift and broadening of the signal of the ^{13}C-labeled carboxyl moiety of the guest molecules is observed for the guest−host complex (Figure 7), similar to the results of ^{13}C NMR spectroscopy in solution (Figure 3).

Intimate contacts between guest and host molecules are also reflected in ^{1}H NMR traces observed via ^{13}C NMR in two-dimensional heteronuclear correlation spectra using proton spin diffusion (Figure 8). The ^{1}H NMR spectrum of the host and the ^{1}H NMR traces from the 2D spectrum without spin diffusion (Figure 8) show the resonance of the adamantyl hydrogens of the host at 2 ppm. Already at a diffusion time of 1 ms, the ^{1}H NMR trace starts to show a significant contribution from the guest protons resonating at 3.5 ppm. At 10 ms the ^{1}H NMR

(23) Additional measurements are available in the Supporting Information: ^{1}H DOSY NMR measurements on the guest molecule and guest−host complexes and the derivation of the association constants (K_a, K_d, and K_b).

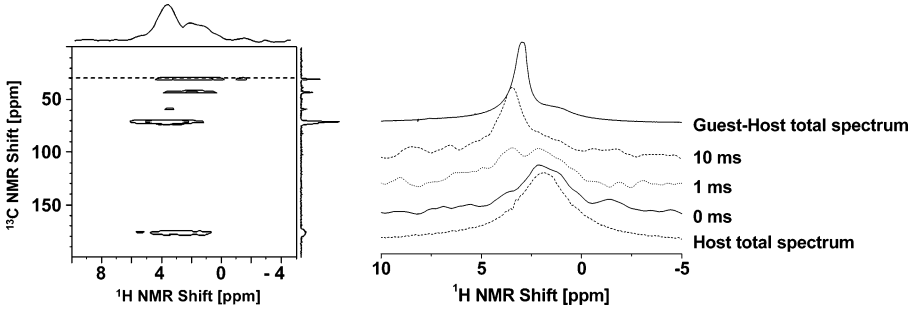

Figure 8. Left: 2D $^{1}H-^{13}C$ NMR correlation spectrum without spin diffusion (the dashed line at 30 ppm shows where the trace was extracted). Right: ^{1}H NMR traces at spin diffusion times of 0, 1, and 10 ms via the 30 ppm ^{13}C NMR resonance of the adamantyl carbons on the periphery of the dendrimer. For comparison the (total) 1D ^{1}H NMR spectra of the guest−host complex (G/H = 32) and the host alone are also shown.

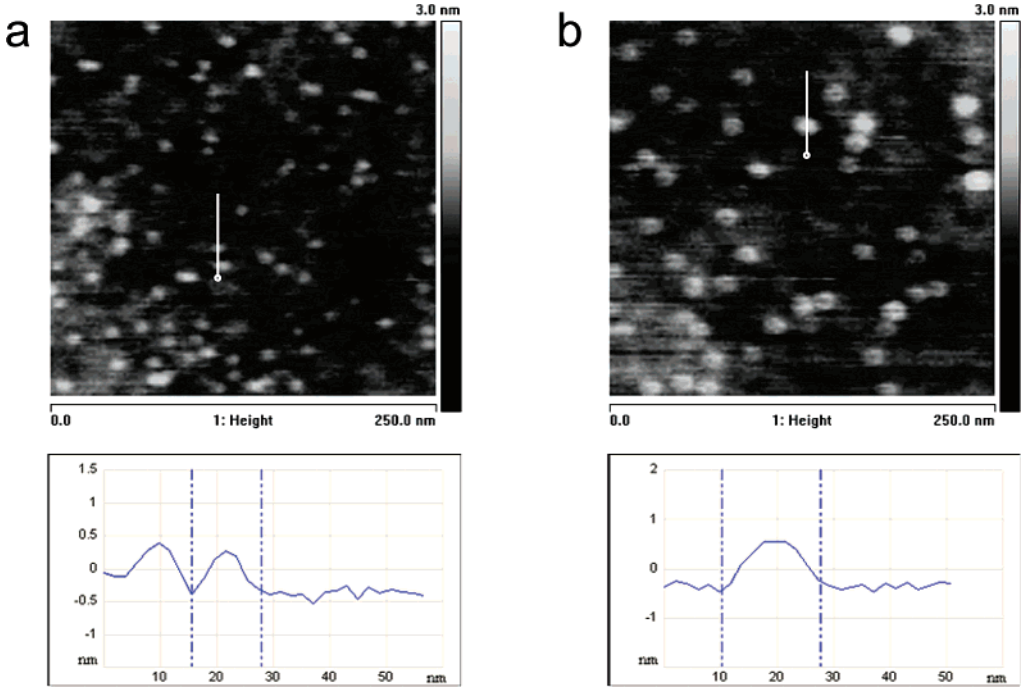

Figure 9. TM-AFM height images (250 × 250 nm) and height traces shown taken along the vertical white line drawn in the images. (a) G/H = 32 at a concentration of 40 pM spun on a silicon substrate. The width of the particle is 12 nm and the height 0.65 nm. (b) Same sample as shown in (a) after annealing in H_2O for 1 h. The width has increased to 18 nm and the height to 1.0 nm.

trace is similar to the overall ^{1}H NMR spectrum of the guest−host complex. Apparently, proton magnetization has already homogeneously diffused over the host and the guest in less than 10 ms. This shows that the system is homogeneous and that the host and guest are intimately mixed.[24]

Tapping mode atomic force microscopy (TM-AFM) was used to study the morphology of the supramolecular complexes in the neat state. When a dilute solution of the single-host complex (G/H = 32, [H] = 40 pM) in chloroform is spun onto a silicon wafer, particles are observed on the silicon surface (Figure 9a) with a height of 0.7 nm and a modal width of approximately 6.5 nm. It is well-known that the aspect ratio of dendrimers is distorted in contact with surfaces.[25] These data agree well with a flattened single-host complex adhered to the substrate surface ($R_{H,\text{by DLS}}$ = 3.0 nm in $CHCl_3$ with 32 bound guest molecules).

When the sample is treated with ultrapure water at room temperature for 1 h (Scheme 3), the single-host complexes start to coalesce (Figure 9b; the modal width is around 9.5 nm and the height 0.9 nm). This is attributed to the fact that the guest molecules are soluble in water, while the host molecules are not. The concomitant dissolution of the guest molecules leads to an exposure of the hydrophobic surface of the host to the aqueous phase. As a consequence the guest-deficient complexes will coalesce to form larger assemblies. The estimated volume of these assemblies is about 3 times larger compared to that of the single-host complexes.

In conclusion, the proton spin diffusion effects observed in 2D $^{1}H-^{13}C$ NMR spectra, combined with the chemical-shift

Scheme 3 [a]

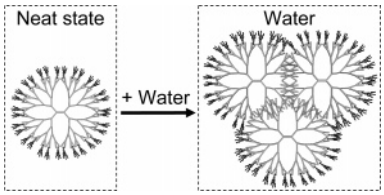

[a] The single-host complexes are dissolved in water and form dendrimer-based assemblies in solution. On a silicon substrate coagulation of the single-host complexes is observed upon annealing in water.

(24) Schmidt-Rohr, K.; Spiess, H. W. *Multidimensional Solid-State NMR and Polymers*; Academic Press: London, 1994.
(25) Tsukruk, V. V.; Rinderspacher, F.; Bliznyuk, V. N. *Langmuir* **1997**, *13*, 2171−2176. Li, J.; Swanson, D. R.; Qin, D.; Brothers, H. M.; Piehler, L. T.; Tomalia, D.; Meier, D. J. *Langmuir* **2000**, *15*, 7347−7350.

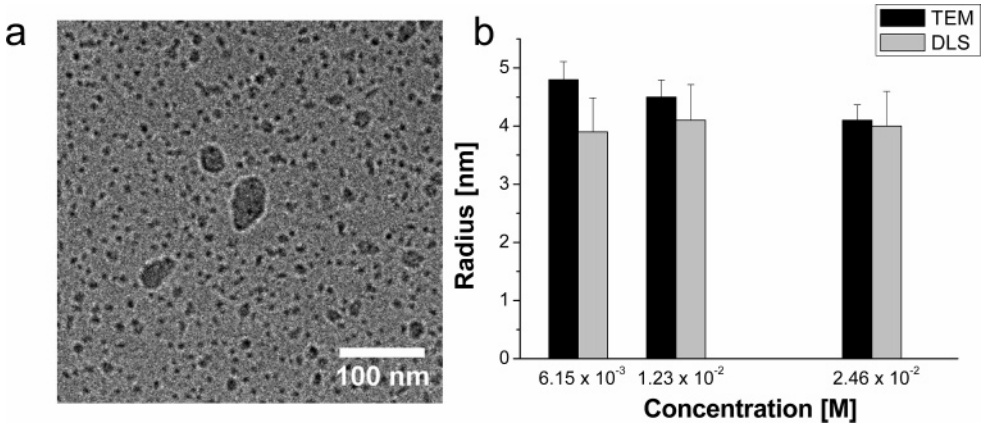

Figure 10. (a) Cryo-TEM image of dendrimer-based assemblies present in water prepared at a concentration of 1.23×10^{-2} M. (b) Radius from image analysis of cryo-TEM images (black bars) and R_H determined by DLS (gray bars).

change and broadening observed in ^{13}C NMR (Figure 7), prove that the single-host complex is still intact in the thin film that remains after evaporation of the chloroform. TM-AFM shows that treatment in water promotes coalescence of several complexes into small assemblies.

Supramolecular Assemblies in Water. The final advancement in the stepwise noncovalent synthetic procedure is going from the neat state to water (Scheme 3). For a sample containing the complex (G/H = 32) at a concentration of 1.23×10^{-2} M, mostly small assemblies with diameters of ~4 nm were observed using cryo-TEM[26] (Figure 10a). Cryo electron tomography after reconstruction of the 3D volume (Supporting Information) showed that the small assemblies were distributed randomly throughout the layer of vitrified water. Also, some larger structures (20−100 nm in size; see Figure 10a) were found embedded in the film.

In DLS (using CONTIN[27]), a dominating fast process (small particles, >95% of the total population) and a slow process (large structures) were observed. The fast process is scattering angle (θ) or $q = (4\pi n/\lambda)\sin(\theta/2)$ (n being the refractive index and $\lambda = 532$ nm the laser wavelength) independent since the I_f/C plot (light scattering intensity divided by the concentration versus q) gives a straight horizontal line (▲; see the lower inset of Figure 11), implying that neither the size nor the shape of the objects can be obtained.

The fast process has a hydrodynamic radius (R_H), calculated from the diffusion constant $D_0 = \Gamma_f/q^2$ (Γ_f being the fast decay in Figure 11) by the Stokes−Einstein equation, similar to the radius calculated from the image analysis of the cryo-TEM images (Figure 10b). The slow process indicates a fractal-like structure (the slope is between −3 and −4 in the I_s/C graph (◇; see the lower inset of Figure 11), with dimensions >1 μm since no plateau at q approaching 0 was found. These structures cannot be observed in cryo-TEM since they do not fit in the layer of vitrified water, which has a thickness of only ~100 nm. The blotting of excess water during sample preparation may disrupt the fractals due to shear forces,[28] leaving behind the structures of 20−100 nm that were observed in cryo-TEM.

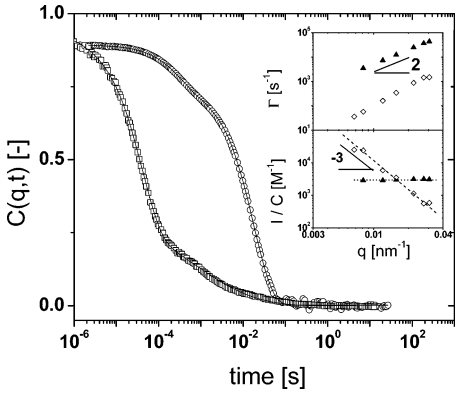

Figure 11. Correlation function $C(q,t)$ obtained by DLS of a sample with G/H = 32 at a concentration of 1.23×10^{-2} M. Decays at two different angles are shown, 150° (□) and 30° (○), both showing a biexponential decay over time which can be analyzed using the CONTIN analysis. The upper inset shows Γ versus q, which has a slope of 2 for both the fast process (▲) and the slow process (◇), meaning normal Brownian motion of the assemblies in solution. The lower inset shows I/C versus q for both the fast and slow processes, yielding q independence for the fast process and fractal-like structures for the slow process (the slope is between −3 and −4 for all concentrations).

At lower concentration, fewer guest molecules would likely be associated, inducing enlargement of the core of the dendrimer-based assemblies, because of an increase in exposed hydrophobic surface of the host molecules. Unexpectedly, the size of the dendrimer-based assemblies is constant irrespective of the concentration (4.1 ± 0.45 nm), and they are stable (for weeks). This combined with the fact that the guest molecules are in fast exchange (by ^{13}C NMR) leads us to conclude that the core of the assembly is kinetically trapped while the guest molecules surrounding the core remain dynamic.

To estimate the number of dendrimers present in the core of the dendrimer-based assembly, molecular dynamics (MD) simulations were performed (Supporting Information). NAMD[29] 2.6 was used to simulate assemblies based on 1−6 dendrimers. In the MD simulations, the aggregates were complexed with 32 guest molecules per dendrimer. The results from the MD studies give a value for the radius of gyration (R_g), while in DLS we measure R_H. Scherrenberg et al. showed with small-

(26) Frederik, P. M.; Hubert, D. H. W. *Methods Enzymol.* **2005**, *391*, 431−448.
(27) Provencher, S. W. *Makromol. Chem.* **1979**, *180*, 201. Provencher, S. W. *Comput. Phys. Commun.* **1982**, 27, 213. Provencher, S. W. *Comput. Phys. Commun.* **1982**, 27, 229.
(28) Magid, L. J.; Gee, J. C.; Talmon, Y. *Langmuir* **1990**, *6*, 1609−1613.
(29) Kalé, L.; Steel, R.; Bhandarkar, M.; Brunner, R.; Gursoy, A.; Krawetz, N.; Phillips, J.; Shinozaki, A.; Varadarajan, K.; Schulten, K. *J. Comput. Phys.* **1999**, *151*, 283−312.

Table 1. Simulated Radius of Gyration by MD ($R_{g,sim}$), Measured R_g by SANS[30] ($R_{g,measd}$), Calculated Hydrodynamic Radius ($R_{H,calcd}$) by Multiplying $R_{g,sim}$ by 1.42, and Measured R_H by DLS ($R_{H,measd}$)[a]

	$R_{g,sim}$ (nm)	$R_{g,measd}$ (nm)	$R_{H,calcd}$ ($1.42R_{g,sim}$) (nm)	$R_{H,measd}$ (nm)
G5-amine[30]		1.39	1.98	1.98
G5-urea-adamantyl (host)	1.53		2.18	2.2
G/H = 55 (32 guests bound on average)	2.06		2.93	2.95

[a] Simulations were performed in vacuo, and DLS measurements in this table were done in chloroform. "G5" refers to the fifth-generation dendrimer.

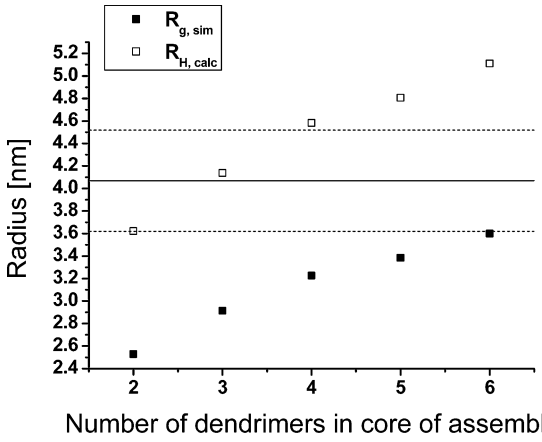

Figure 12. Results from molecular dynamics studies showing the simulated R_g ($R_{g,sim}$) and the calculated R_H ($1.42R_{g,sim}$). The horizontal line shows the average radius (R_{av} = 4.1 ± 0.45 nm), while the two dashed horizontal lines show the upper and lower limits, calculated by averaging DLS measurements. The dendrimer-based assembly with three host molecules in the core is closest to what was observed experimentally.

angle neutron scattering (SANS) that for a fifth-generation poly(propylene imine) dendrimer $R_H = 1.42R_g$.[30] They also concluded that there was no influence of solvent or end-group modifications. The applicability of this relation to our system was investigated by comparing simulations and DLS measurements in chloroform (Table 1).

For the host molecule in chloroform, the calculation of $R_{H,calcd}$ is accurate (second row of Table 1) compared to the measured value ($R_{H,measd}$). A sample with a G/H = 55 in chloroform will have on average 32 guest molecules associated (determined by ^{13}C NMR at this concentration). The calculated R_H ($R_{H,calcd}$) in vacuo simulated with 32 guests around the host also corresponds well to the measured value ($R_{H,measd}$) in chloroform. Despite the fact that the guest molecules collapse onto the host in vacuo and are solvated in chloroform solution, the simulation and DLS results correspond surprisingly well, using the relation $R_{H,calcd} = 1.42R_{g,sim}$. We expect this relation also to hold in water, since the solvation behavior of the guest in chloroform and that in water are comparable (the R_H values of the guest are similar in chloroform and in water[31]). To get an idea of how many host molecules are assembled in the core of a dendrimer-based assembly with the measured R_H, a series of MD simulations is performed. In Figure 12, the $R_{g,sim}$ values and $R_{H,calcd}$ values are plotted versus the number of host molecules present in the core of the assemblies.

By combining the MD simulations with the DLS and cryo-TEM analyses, we find the supramolecular assembly consisting of three dendrimers in the core to be the most abundant. Nevertheless, the solutions contain a distribution of particle sizes, in which assemblies with more or fewer dendrimers in the core are also present.

In summary, after completion of the noncovalent synthetic procedure, surprisingly stable small dendrimer-based assemblies are formed in water which have a kinetically trapped core of on average three host molecules and a dynamic corona consisting of multiple guest molecules, unlike the single-host complexes observed in chloroform.

Conclusions

We have presented an in-depth analysis of a stepwise noncovalent synthetic procedure used to obtain dendrimer-based guest−host assemblies in water. This synthetic approach involves first a preassembly step in chloroform. In this step, the host is not aggregated and a fraction of the guest molecules is bound to it (yielding a single-host complex), according to the association constant (K_b), which is concealed by guest self-association. The value for K_b is therefore higher than previously reported. When the chloroform is evaporated, a thin film remains, in which all guest molecules are bound to the host. Upon dissolution of the single-host complexes in water, mainly small dendrimer-based assemblies are formed with a diameter of 4.1 ± 0.45 nm. Although simulations were used to estimate the core of the new assemblies in water to consist of on average three dendrimers, we have no explanation yet why these sizes are found irrespective of the concentration. This concentration independence indicates that the core of the dendrimer-based assemblies is kinetically trapped upon dissolution in water. Apparently, hydrophobic forces and shielding of the host by the hydrophilic guest molecules are optimal at these distinct numbers of host molecules in the core of the assembly. The corona of the dendrimer-based assemblies in water, consisting of multiple guest molecules, is dynamic. Transition of the neat state to water was further investigated using AFM. These experiments showed that upon addition of water indeed the single-host complexes have a tendency to coalesce together. In conclusion, we have shown that the concepts of stepwise noncovalent synthesis provide valuable tools to obtain new supramolecular assemblies.

Experimental Section

Solution NMR. For a typical NMR sample with G/H = 32 and a guest concentration of 2.46×10^{-2} M in chloroform, 7.11 mg of the host (M_w = 18511.82 g/mol) and 10 mg of the guest molecule (M_w = 813.9 g/mol) were dissolved together in 0.5 mL of $CDCl_3$ and stirred for 2 min (vortex). In the titration experiment, the guest concentration was kept constant and the guest/host ratio was changed by adding more and more of the host. For the dilution experiments, the guest/host ratio was constant and the concentration was lowered by adding $CDCl_3$. ^{13}C NMR measurements were performed on a Varian Unity Inova 500 spectrometer operating at 500.618 MHz equipped with a 5 mm 500 SW/PFG probe from Varian at 25 °C. ^{13}C NMR chemical shifts were measured using an insert tube filled with TMS (set at exactly 0 ppm). ^{1}H DOSY NMR measurements were done without the insert. ^{1}H DOSY was performed using a 5 mm 500 ID/PFG probe from Varian at 25 °C.

(30) Scherrenberg, R.; Coussens, B.; P. van Vliet, Edouard, G.; Brackman, J.; de Brabander, E.; Mortensen, K. *Macromolecules* **1998**, *31*, 456−461.
(31) $R_{H,guest}^{water}$ = 0.73 nm and $R_{H,guest}^{chloroform}$ = 0.58 nm (both determined by ^{1}H DOSY NMR at a concentration below 10^{-3} M, where the guest is molecularly dissolved in chloroform as well as in water).

Solid-State NMR. ^{1}H-decoupled ^{13}C NMR spectra were recorded on a Bruker DMX500 spectrometer with a ^{13}C NMR frequency of 125.13 MHz. A 4 mm MAS probehead was used with a sample rotation rate of 8 kHz. The radio frequency power was adjusted to obtain 5 ms 90° pulses for both the ^{1}H and ^{13}C nuclei. All ^{13}C NMR spectra were recorded by using standard ^{1}H−^{13}C cross-polarization with an amplitude-modulated contact pulse of 1 ms. For 2D ^{1}H−^{13}C CPMAS spectra, we used the standard WISE pulse sequence with a ramped contact pulse.

Tapping Mode Atomic Force Microscopy. A 40 pM solution of the host or the single-host complex (G/H = 32) was spin-coated at 1000 rpm for 15 s. AFM was performed on a Dimension 3100 (Digital Instruments). Standard silicon cantilevers (NSG10, 190−325 kHz, and NSG01, 115−190 kHz, tips from NT-MDT) were used.

Dynamic Light Scattering. The samples of the small dendrimer-based assemblies in water were made by first preparing a solution of 7.11 mg of the host and 10 mg of the guest together in 1 mL of $CHCl_3$. After 2 min of stirring (vortex) the chloroform was evaporated using a gentle stream of nitrogen gas (over the course of 1 h). Afterward the thin film was dried in a vacuum oven for 30 min at room temperature. The thin film was subsequently dissolved in 0.5, 1, or 2 mL of ultrapure water to obtain a final concentration of 6.15×10^{-3}, 1.23×10^{-2}, or 2.46×10^{-2} M, respectively.

The time autocorrelation function of the scattered intensity $G(q,t)$ was determined with the aid of an ALV-5000/E fast multi-τ correlator in the time range 10^{-7}−10^3 s from which the relaxation function $C(q,t) = [(G(q,t) - 1/f^*]^{1/2}$ was computed ($f^* < 1$ is the instrumental known factor) at a constant scattering wave vector **q**. $C(q,t)$ shows two distinct decays with diffusive (q^2-dependent) rates (Γ_f, Γ_s) obtained from the CONTIN analysis. The hydrodynamic radius (R_H) was extracted from the measured diffusion coefficient D_0 ($=\Gamma_f/q^2$) assuming validity of the Stokes−Einstein relation, $R_H = kT/6\pi\eta D$ (k being the Boltzmann constant and η the solvent viscosity), for spherical objects.

Cryogenic Transmission Electron Microscopy. Samples identical to those used for DLS were used. The measurements were performed on an FEI Tecnai 20, type Sphera TEM instrument equipped with an LaB6 filament operating at 200 kV. Images were recorded with a bottom-mounted 1K × 1K Gatan CCD camera. A Gatan cryoholder operating at ∼−170 °C was used for the cryo-TEM measurements. The sample vitrification procedure was carried out using an automated vitrification robot (FEI Vitrobot Mark III). TEM grids, both 200 mesh carbon-coated copper grids and R2/2 Quantifoil Jena grids, were purchased from Aurion. The Quantifoil grids were surface plasma treated using a Cressington 208 carbon coater operating at 5 mA for 40 s prior to the vitrification procedure. Cryotomography measurements were performed on an FEI Titan Krios equipped with a field emission gun (FEG) operating at 300 kV. Images were recorded using a Gatan GIF energy filter and a 2K × 2K Gatan CCD camera. The tomography reconstruction was performed using the Inspect3D (FEI Co.) software program, version 2.1.

Cryo-TEM Images. Image analysis was done using the SPIDER/WEB software package (Wadsworth) for the image obtained from a Sphera electron microscope (FEI), and ImageJ (http://rsb.info.nih.gov/ij/) was used to analyze the high resolutions from a Titan electron microscope (FEI). See also the Supporting Information.

Molecular Dynamics. Using NAMD 2.6, molecular dynamics simulations were performed. See the Supporting Information.

Acknowledgment. We thank Jeroen van Herrikhuijzen for providing PEG-coated gold nanoparticles used in the tomography experiment for reconstruction. We are grateful to Felix de Haas for helping with the SPIDER script for the cryo-TEM image analyses.

Supporting Information Available: Derivation of dimerization and binding equilibria, ^{1}H DOSY NMR analysis of guest−host binding, image analysis of cryo-TEM images, tomography reconstruction, and details of the molecular dynamics simulations (PDF, MPG). This material is available free of charge via the Internet at http://pubs.acs.org.

JA074991T